Using high spatial resolution to improve BOLD fMRI detection at 3T

Juliana Iranpour, Gil Morrot, Béatrice Claise, Betty Jean, J.-M. Bonny

PLOS | ONE

RESEARCH ARTICLE

Using High Spatial Resolution to Improve BOLD fMRI Detection at 3T

Juliana Iranpour[1☯], Gil Morrot[2☯], Béatrice Claise[3‡], Betty Jean[3‡], Jean-Marie Bonny[1☯*]

1 UR370 QuaPA—INRA, F-63122, Saint-Genès-Champanelle, France, **2** Laboratoire Charles Coulomb—UMR 5221 CNRS, Université des Sciences et Techniques—Montpellier 2, place Eugène-Bataillon, 34090, Montpellier, France, **3** Neuroradiologie A, Plateforme Recherche IRM—CHU Gabriel-Montpied, F63000, Clermont-Ferrand, France

☯ These authors contributed equally to this work.
‡ These authors also contributed equally to this work.
* jean-marie.bonny@clermont.inra.fr

Citation: Iranpour J, Morrot G, Claise B, Jean B, Bonny J-M (2015) Using High Spatial Resolution to Improve BOLD fMRI Detection at 3T. PLoS ONE 10(11): e0141358. doi:10.1371/journal.pone.0141358

Editor: Pew-Thian Yap, University of North Carolina, UNITED STATES

Received: August 24, 2015

Accepted: October 7, 2015

Published: November 9, 2015

Data Availability Statement: All relevant data are within the paper.

Funding: This work was supported by Contrat AIB 23000400, Conseil régional d'Auvergne (http://www.auvergne.fr/) and European Funds for Regional Development (http://en.europe-en-france.gouv.fr/), to JI; and AIC AromaSalt, Science and Process Engineering of Agricultural Products (http://www.cepia.inra.fr/en), to JMB. The funders had no role in study design, data collection and analysis, decision to publish, or preparation of the manuscript.

Competing Interests: The authors have declared that no competing interests exist.

Abstract

For different functional magnetic resonance imaging experiments using blood oxygenation level-dependent (BOLD) contrast, the acquisition of T_2*-weighted scans at a high spatial resolution may be advantageous in terms of time-course signal-to-noise ratio and of BOLD sensitivity when the regions are prone to susceptibility artifacts. In this study, we explore this solution by examining how spatial resolution influences activations elicited when appetizing food pictures are viewed. Twenty subjects were imaged at 3 T with two different voxel volumes, 3.4 μl and 27 μl. Despite the diminution of brain coverage, we found that high-resolution acquisition led to a better detection of activations. Though known to suffer to different degrees from susceptibility artifacts, the activations detected by high spatial resolution were notably consistent with those reported in published activation likelihood estimation meta-analyses, corresponding to taste-responsive regions. Furthermore, these regions were found activated bilaterally, in contrast with previous findings. Both the reduction of partial volume effect, which improves BOLD contrast, and the mitigation of susceptibility artifact, which boosts the signal to noise ratio in certain regions, explained the better detection noted with high resolution. The present study provides further evidences that high spatial resolution is a valuable solution for human BOLD fMRI, especially for studying food-related stimuli.

Introduction

With the widespread use of high magnetic fields, interest in increasing the spatial resolution in fMRI is constantly developing. While ultra-high field allows new levels of spatial resolution and specificity to be achieved [1, 2], it also makes sense to reduce the voxel volume (V) of gradient-echo echo-planar imaging (EPI) scans at less intense static fields, which are still those most commonly encountered. Some multi-resolution fMRI studies have indeed converged in demonstrating a better ability to detect neural activation in specific regions by acquiring high-

resolution scans at 3 T; *e.g.* with $V = 6.4–8.0$ μl in amygdala [3, 4] or with $V = 2.1$ μl in brainstem [5].

The expected benefits of the voxel volume reduction are twofold. Firstly, it is a straightforward solution to mitigate BOLD-sensitivity modulations due to susceptibility artifacts [6–8]. When voxel size is reduced isotropically, its efficiency is furthermore not prone to the orientation of magnetic field gradients, known to change rapidly over the brain. Secondly, it may be advantageous in terms of time-course signal-to-noise ratio (tSNR) to acquire images with a reduced voxel volume, in which thermal noise dominates. In this regime, tSNR comes closer to what can be expected from the SNR of an individual image. Moreover tSNR increases steadily with the degree of smoothing, rather than being limited when physiological fluctuations with time dominate [9–11].

The voxel volume separating thermal noise and physiological noise dominance regimes has been determined experimentally: $V = 5.8$ μl for gray matter at 3 T with a 16-channel detector array head coil [12]. Thus it is suggested that a voxel volume far below the commonly used values, which are around 27 μl at 3 T, be used. Accordingly we compared activations elicited by viewing food pictures in two scanning conditions differing only in the voxel volume of acquisition at 3 T using two widely different isotropic volumes, 3.4 μl and 27 μl. Viewing food pictures is known to activate a large set of visual, gustatory and reward processing areas [13–27] that suffer to different degrees from susceptibility artifacts, such as occipital lobe, orbitofrontal cortex (OFC), amygdala or insula. Also, the results of two recent meta-analyses can provide useful normative data [28, 29] to assess the effect of voxel volume reduction, provided the examined experiments have been performed using a coarse voxel volume, corresponding unequivocally to a physiological noise dominant regime. In support, Table 1 records the voxel volume used in

Table 1. Voxel volume, magnetic field strength and echo time of studies included in the meta-analyses [28, 29] on the neural correlates of processing visual food cues.

Reference	Voxel volume (μl)	Field (T)	Echo time (ms)
[30]	10.1	1.5	60
[17]	27.0	1.5	40
[31]	27.0	1.5	50
[32]	32.7	1.5	40
[33]	36.0	1.5	30
[34]	36.0	1.5	40
[22]	36.0	1.5	50
[14]	46.2	1.5	40
[23]	48.1	1.5	40
[27]	64.0	1.5	40
[15, 16]	67.3	1.5	40
Mean	**39.1**	**1.5**	**42.7**
[35]	27.0	3	30
[25]	27.0	3	40
[36]	27.0	3	30
[37]	33.1	3	30
[21]	36.0	3	30
[24]	54.9	3	25
[19, 20]	57.8	3	30
[18]	60.8	3	27
Mean	**40.4**	**3.0**	**30.3**

doi:10.1371/journal.pone.0141358.t001

all the studies included in the meta-analyses, showing that $V \geq 27$ μl for 20 out of 21 of them, and for all those at 3 T.

We hypothesized that the high spatial resolution (HR) protocol could reveal more significant and spatially-specific activations in response to viewing pictures of food in normal-weight subjects. In order to capitalize on the improved ability of high spatial resolution fMRI data to resolve fine spatial structures [38], it is necessary to adapt the width of the smoothing kernel to the true size of activation and to the contrast-to-noise ratio [39], both being *a priori* unknown. This is why both datasets were analysed using different smoothing sizes for selecting the appropriate coarser resolution in any anatomical region-of-interest (ROI).

Lastly, a 32-channel head coil was used in our study, which is theoretically more sensitive than the 16-channel one used by Bodurka *et al.* [12]. It is thus likely that the voxel volume that splits the thermal noise and physiological noise dominance regimes at 3 T may be lower than 5.8 μl for gray matter, *i.e.* rather close to the voxel volume used in the HR condition. That is why, to clarify the reasons for any improved activation detection, normalized maps of the baseline signal and of the noise were calculated at both voxel volumes. They were used to assess separately the effect of voxel volume reduction on the amplitudes of the susceptibility artifacts and of the physiological noise. Under these conditions, the question on how voxel size is affecting the sensitivity in BOLD-based fMRI at high field can be fully addressed.

Methods

Subjects

Twenty healthy, right-handed volunteers participated in this study (11 female, mean age ± SD = 25 ± 2 years; 9 male, mean age ± SD = 26 ± 2 years). All confirmed that they had no clinical history of major disease, and a normal eating behavior using the screening test for eating behavior disorders [40]. Hunger being known to modulate the response of certain areas to food pictures, the participants were food-restricted and were allowed to drink only water for 2 h before the fMRI session.

The study was approved by the ethics committee of the university hospital of Clermont-Ferrand (AU 993). Written informed consent from all the subjects was obtained before the experiment, in accordance with the Declaration of Helsinki.

Stimulation paradigm

The stimulation paradigm consisted of alternating blocks presenting, in a randomized order, either ready-to-eat edible objects, or pictures of items that were clearly unrelated to food (see Fig 1). A fixation cross was presented in the center of the screen between two pictures in order to avoid saturation. In all, 54 different pictures were selected for each of the food-related and nonfood-related blocks. The food images depicted savory and sweet meals commonly served at breakfast, lunch and dinner. Images were presented to each of the subjects in randomized order. Pictures were presented using E-Prime 2.0 software (Psychological Software Tools, Sharpsburg, USA) via an MR-compatible visual stimulation system (NordicNeuroLab, Bergen, NO).

After an fMRI session, all the participants were asked to rate each picture showing food for motivational salience on a 7-point scale (0: extremely repulsive; 1: very repulsive; 2: quite repulsive; 3: neutral; 4: quite appetizing; 5: very appetizing; 6: extremely appetizing). The mean ± SD of these post-scanning ratings was 4.5 ± 1.2, significantly higher than 4 (paired Student's t-test: $t\,(54) = 12.2$, $p < 0.001$), thus indicating that our subjects rated the pictures showing food as significantly appetizing.

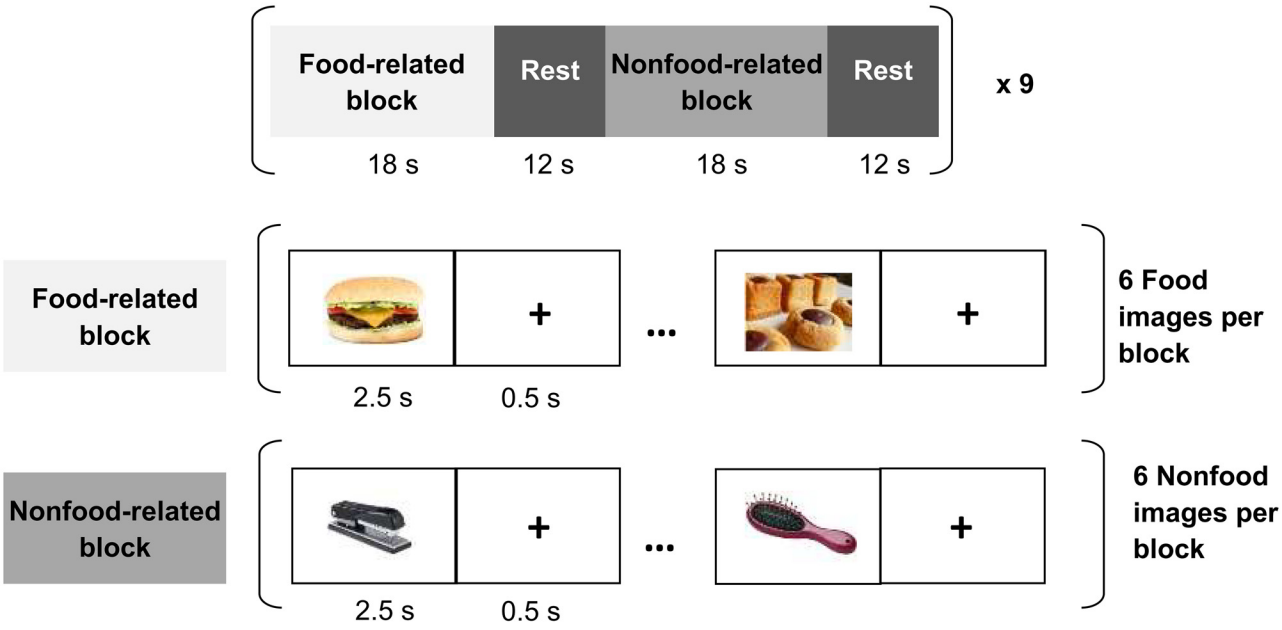

Fig 1. Graphical outline of the stimulation protocol used in this fMRI experiment. Stimuli were presented according to a block design involving food-related and non-food-related blocks. During the presentation of food images, participants were asked to imagine the taste of the viewed food, as if they were actually eating it. Each image was separated by a fixation cross and a rest period was placed between two blocks.

doi:10.1371/journal.pone.0141358.g001

Data acquisition

The imaging data were collected on a 3 T General Electric Discovery MR750 MRI system (General Electric Medical Systems, Milwaukee, USA). A 32-channel receive-only phased-array head coil was used for brain imaging.

A T_1-weighted inversion-recovery-prepared fast 3D gradient-echo sequence (BRAVO) was employed to obtain anatomical images of the whole brain of each subject. The acquisition parameters were: flip angle = 12°, inversion time = 400 ms, repetition time (TR) = 8.8 ms, echo time (TE) = 3.5 ms. The whole brain volume was covered at high-resolution using field-of-view = 240 × 192 × 175 mm^3 and matrix 288 × 288 × 146 (*i.e.* voxel volume = 0.8 × 0.7 × 1.2 mm^3, ∼ 0.7 μl).

Two functional experiments were conducted with the same paradigm, but differing in their voxel volume only. T_2^*-weighted gradient-echo images were collected using a 2D single-scan EPI sequence (TR = 3000 ms and flip angle = 90°). TE = 30 ms was chosen according to Table 1. Array spatial sensitivity encoding a parallel imaging option was activated for its ability to decrease the geometric distortion in EPI, the regions with inhomogeneous magnetic field being prone to such artifacts.

The low resolution (LR) dataset was obtained in axial orientation parallel to the anterior commissure-posterior commissure line with an isotropic 3 × 3 × 3 mm^3 = 27 μl voxel volume (50 interleaved contiguous slices, field-of-view = 192 × 192 mm^2, matrix = 64 × 64, reception bandwidth = 250 kHz, phase encoding along the anterior-posterior direction). The HR dataset was acquired in the same orientation with an 8 times lower voxel volume equal to 1.5 × 1.5 × 1.5 mm^3 = 3.4 μl (42 interleaved contiguous slices, field-of-view = 192 × 192 mm^2, matrix = 128 × 128, reception bandwidth = 250 kHz, phase encoding along the anterior-posterior direction). The 150 mm thick block was sufficient to cover the whole brain, but higher resolution with the same TR limited the coverage to 63 mm (see Fig 2). This acquisition volume

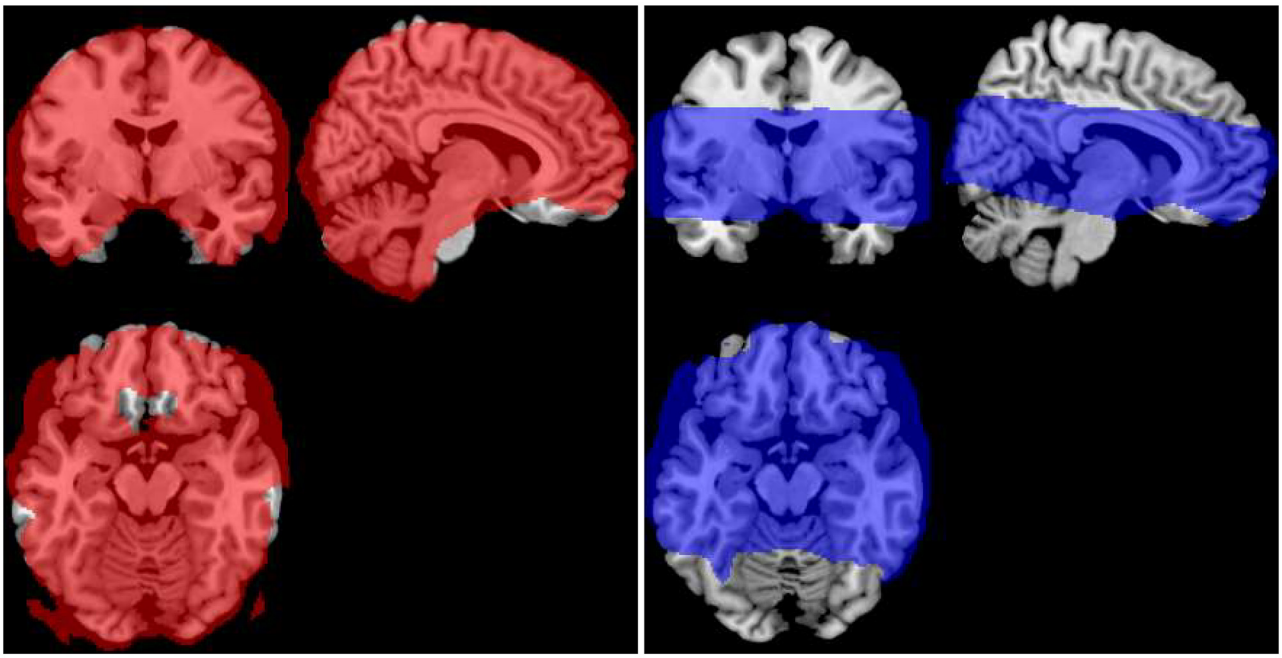

Fig 2. Masks showing the voxels contributing to the group analysis for the two conditions.

doi:10.1371/journal.pone.0141358.g002

ranged from $z = -27$ to 36 mm in Montreal Neurological Institute (MNI) space, which suffices for intercepting all brain regions known to be elicited when viewing food pictures [28, 29].

Each subject completed the same paradigm twice, the images being acquired in LR and HR conditions in a randomized order. Both consisted of the acquisition of 180 successive brain volumes.

Data analysis

The fMRI datasets were preprocessed and analysed using SPM8 (Statistical Parametric Mapping, Wellcome Department of Cognitive Neurology, London, UK) implemented in Matlab (MathWorks Inc., Natick, USA). The analysis relative threshold *defaults.mask.thresh* (SPM default = 0.8) was decreased to 0.2 so that the voxels belonging to regions with signal dropout could contribute to the analysis whereas the background voxels were still excluded.

Images were firstly corrected for slice timing using the middle slice as reference. Secondly, images were realigned to the first image with a six-parameter rigid-body spatial transformation to correct for head motion. Thirdly, the anatomical scan was coregistered with the mean of realigned functional images after setting the origin of both the functional and the anatomical scans to the AC. The *New Segment* function was applied to segment anatomical images into gray matter, white matter and other tissues. The DARTEL warping method (high-dimensional Diffeomorphic Anatomical Registration Through Exponentiated Lie algebra) [41] was used to create flow fields specific to our subjects. The template was affine registered in MNI space. The functional images were normalized using compositions of flow fields (*i.e.* nonlinear

deformations for warping all subject-specific images to the template) and template affine transformation parameters.

Fourthly, the normalized images of both LR and HR functional datasets were spatially smoothed with an isotropic Gaussian kernel of different sizes, expressed by the full width half-maximum (FWHM) in mm. FWHM ranged from 1.5 mm to 8 mm for the HR dataset, from 2.5 mm to 8 mm for the LR one, with a step of 0.5 mm. The maximum FWHM corresponds to 2–3 times the voxel size of the LR dataset as usually chosen [42].

For each subject, conditions and Gaussian kernel sizes (*i.e.* 20 x 2 x (12 + 14) = 1040 datasets), first-level statistical parametric maps were first generated using the general linear model to describe the variability of the data on a voxel-by-voxel basis. The model consisted of a boxcar function, using the food-related and non-food-related blocks as regressors of interest, convolved with the canonical SPM hemodynamic response function. The contrast between viewing food and non-food pictures was then generated.

Subsequently, a second-level group random effects analysis was performed to subject this contrast to a one-sample *t*-test. A cluster was chosen for its significance in two steps; using a primary voxel-level thresholding at a level p_p and by evaluating the cluster-level FDR-corrected *p*-value (Q_{FDR}), which gives the family-wise error rate probability (*i.e.* the level of false-positives in the cluster) due to multiple comparisons [43]. p_p was set to 0.001 to avoid false positives and lack of specificity [44] and a cluster was considered as significant when Q_{FDR} was less than 0.05. No minimum size of contiguous voxels was required.

The obtained clusters were inspected in several anatomical ROIs specified by the Automated Anatomical Labeling (AAL) atlas [45]. The most concurrent regions activated in response to viewing food pictures were selected according to the meta-analyses [28, 29], *i.e.* fusiform gyrus, middle and superior occipital gyrus, lingual gyrus, lateral OFC (Frontal Mid Orb), insular cortex and amygdala. The parietal gyrus was not investigated because this region was outside the covered block in HR condition.

For analysing the effect, smoothing and selecting an appropriate FWHM in a given ROI, the selected value of FWHM was the lowest leading to a significant cluster. This choice is justified by the concern of obtaining less extensive clusters, so better localized, and prevents regions that are functionally different from merging together [46].

For further analysis at the individual level of the sensitivity differences between the two conditions LR and HR, three metrics were evaluated in several anatomical ROI. Firstly, the 95th percentile measures of the percent signal change (PSC) was calculated in order to quantify a BOLD variation representative of the typically active voxels within the ROI. Secondly, the baseline mean signal and the standard deviation of noise were also mapped from the 42 images of the EPI time-series acquired during the rest periods. To neutralize the between-subject changes of mean signal intensity, these individual maps were then intensity-normalized using the signal of the cerebral peduncle (delineated by the JHU white-matter atlas) as a reference. Finally, baseline mean signal and standard deviation of noise were averaged within each anatomical ROI.

To compare the means of PSC, baseline signal and noise obtained in the two conditions, paired-sample two-tailed Student's *t*-test or Wilcoxon signed-rank tests were applied according to a prior Shapiro test for normality. All these statistical analyses were carried out with the open source R Studio Software (http://www.rstudio.com/).

Results

The brain regions activated at the group level for the contrast between viewing food and non-food pictures are represented in Table 2 for both LR and HR conditions, and visually compared

Table 2. Locations (MNI) of activated brain regions at the group level for the contrast between viewing food and non-food pictures obtained from HR data. The reported clusters were thresholded at the same $p < 0.001$ (uncorrected for multiple comparisons). Q_{FDR} indicates the level of FDR on clusters.

Brain region	HR						LR					
	Brodmann area	Volume (K_E)	x, y, z (mm)	t	Q_{FDR}	Smoothing (mm)	Brodmann area	Volume (K_E)	x, y, z (mm)	t	Q_{FDR}	Smoothing (mm)
L Amygdala	34	9	-26, 0, -18	4.26	0.039	1.5	-	-	-	-	-	-
	34	14	-20, -3, -18	4.69	0.008	1.5	-	-	-	-	-	-
R Amygdala	34	20	23, 2, -17	5.69	0.005	1.5	34	51	18, 0, -17	5.12	0.016	2.5
L Frontal Mid Orb	11	29	-23, 35, -18	4.97	0.000	1		-	-	-	-	-
R Frontal Mid Orb	11	6	26, 35, -21	5.43	0.045	1		-	-	-	-	-
L Insula	13	61	-36, -10, 13	5.45	0.000	1	13	140	-41, -9, 6	6.38	0.000	2.5
	38	7	-44, 6, -8	4.95	0.029	1	13/38	42	-39, 3, -11	4.79	0.03	2.5
	13/22	11	-44, 3, -2	4.83	0.006	1		-	-	-	-	-
	13	6	-39, 0, -11	4.22	0.045	1		-	-	-	-	-
R Insula	13	27	40, -3, 4	5.74	0.000	1		-	-	-	-	-
	13	7	39, 5, -12	5.1	0.029	1		-	-	-	-	-
	38	9	45, 12, -8	4.86	0.013	1		-	-	-	-	-
L Fusiform	19	20	-29, -75, -9	4.65	0.000	1	19	330	-27, -61, -15	6.91	0.000	2.5
		-	-	-	-	-	19	35	-29, -57, -8	5.51	0.003	2.5
		-	-	-	-	-	19	16	-24, -51, -14	4.75	0.035	2.5
R Fusiform	19	15	27, -52, -11	5.56	0.006	1	19	968	23, -78, -14	8.54	0.000	2.5
L Lingual	17/18	12	-14, -88, -5	4.69	0.004	1	17/18	1315	-5, -82, -2	9.1	0.000	2.5
R Lingual	17	19	11, -88, -3	5.71	0.005	1.5	17/18	1312	11, -84, -11	11.36	0.000	2.5
		-	-	-	-	-	19	68	29, -54, -6	6.1	0.007	2.5
L Occ mid	18/19	71	-29, -82, 12	7.31	0.000	1		-	-	-	-	-
	18/19	108	-18, -96, 7	6.19	0.000	1	18/19	1240	-17, -96, 6	7.99	0.000	2.5
	18/19	12	-38, -78, 4	5.78	0.004	1		-	-	-	-	-
	18/19	56	-29, -82, 1	5.68	0.000	1		-	-	-	-	-

(*Continued*)

Table 2. (*Continued*)

Brain region	HR						LR					
	Brodmann area	Volume (K_E)	x, y, z (mm)	t	Q_{FDR}	Smoothing (mm)	Brodmann area	Volume (K_E)	x, y, z (mm)	t	Q_{FDR}	Smoothing (mm)
	18/19	9	-24, -73, 25	5.5	0.013	1		-	-	-	-	-
R Occ mid	18/19	59	34, -85, 12	5.58	0.000	1		-	-	-	-	-
	18/19	7	28, -91, 7	4.79	0.029	1	18/19	694	27, -94, 10	8.22	0.000	2.5
	18/19	6	24, -93, 4	4.77	0.045	1		-	-	-	-	-
L Occ sup	17	55	-11, -96, 1	5.72	0.000	1	17/18	309	-15, -93, 4	7.15	0.000	2.5
	19/7	36	-20, -69, 37	5.23	0.000	1	19/7	132	-26, -67, 39	5.86	0.000	2.5
		-	-	-	-	-	19/7	143	-23, -76, 42	7.58	0.000	2.5
R Occ sup	18	13	23, -88, 10	4.77	0.004	1	18/19	244	26, -94, 12	7.79	0.000	2.5
		-	-	-	-	-	19/7	211	27, -70, 37	5.86	0.000	2.5

doi:10.1371/journal.pone.0141358.t002

in Fig 3. For the same significance threshold ($Q_{FDR} < 0.05$), more regions were found significantly activated with the HR imaging protocol than with the LR one. Bilateral activation of the lateral OFC was detected only in the HR condition. Moreover the insula and amygdala that were significantly activated unilaterally in the LR condition, reached bilateral significance in the HR condition (Table 2, Fig 3).

The fMRI activation metrics are listed in Table 3 for the two conditions LR and HR. Essentially, this showed that PSC is greater under HR conditions for all the studied regions except the right lateral OFC (Frontal Mid Orb). The baseline signal is significantly stronger under HR in the mygdala and the OFC, while the noise is weaker under HR only in the left OFC.

Discussion

In this fMRI study, we examined the characteristics of brain activations elicited by viewing food cues compared with non-food ones using two imaging protocols that differ only in the voxel volume of the scans. These kinds of paradigm are known to lead to a low inter-study reproducibility since only 12 to 41% of the experiments contributed to the clusters [29].

In conditions of similar resolutions (LR), the activations detected in our study recover only a part of the activations described by the meta-analyses [28, 29], in particular no activation was found in left amygdala, left lateral OFC, and right insula. A lack of sensitivity undoubtedly explains the low inter-study reproducibility reported in the meta-analyses and justifies using the possibly more sensitive conditions of HR.

All the activations reported in the meta-analyses occurred under our HR conditions, at a high level of statistical significance. The Q_{FDR} found was often much lower than the conservative threshold of 0.05. This point deserves to be emphasised since the activations revealed by meta-analysis are generally more robust, being less prone to false alarms, because these errors will not be replicated across studies [47].

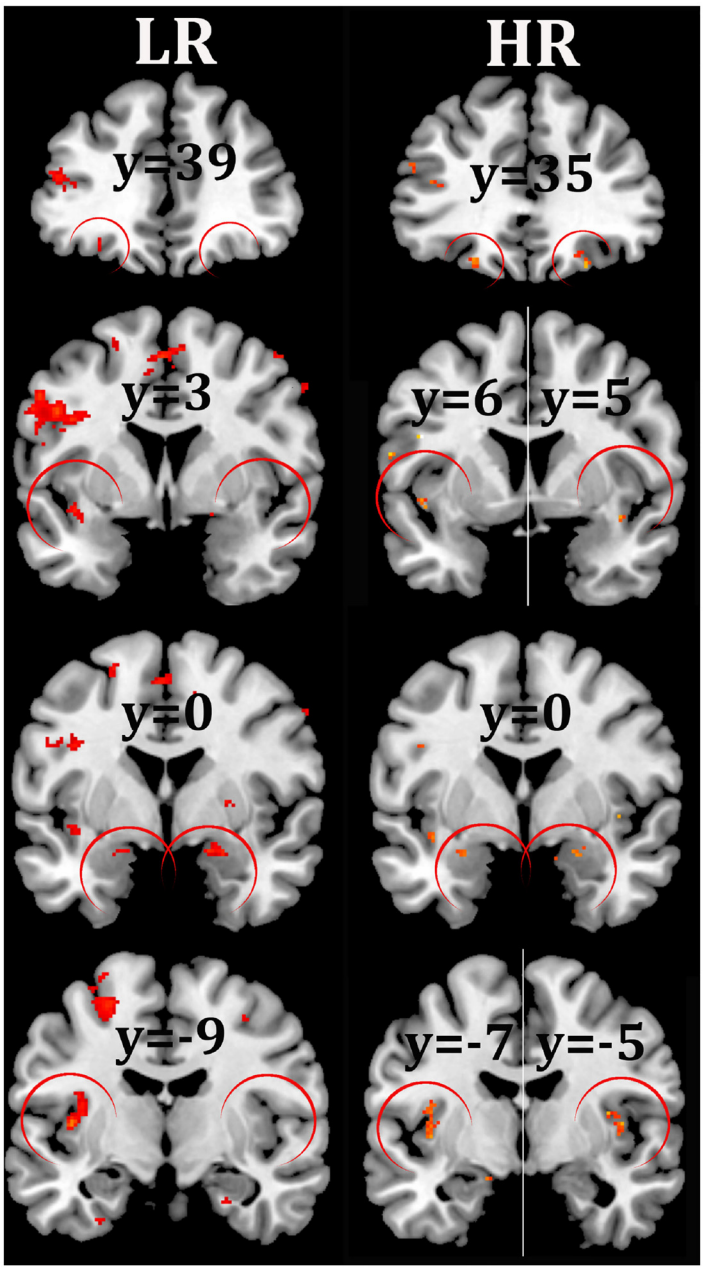

Fig 3. Group statistical parametric maps for the comparison of significantly activated regions detected under LR and HR conditions for the contrast between viewing food and non-food pictures. Activations were successively shown in the OFC (y = 35/39), anterior insula (y = 3/6), amygdala (y = 0) and insula (y = -5/-9) using a voxel-wise p<0.001 uncorrected threshold, with an extent threshold of 5 voxels (neurologic orientation, right-on-right). Under such conditions, the activations observable in the left amygdala and right OFC with LR do not resist to the $Q_{FDR} < 0.05$ threshold used in Table 2.

doi:10.1371/journal.pone.0141358.g003

In addition, these results show that activations that are unilateral in the meta-analyses are found as bilateral under HR conditions. Firstly, the lateral OFC (Frontal Mid Orb) which was found activated on the left [MNI (−26, 32, −14) in [29] and MNI (−25, 31, −17) in [28]] was bilaterally activated in our HR condition [MNI (−23, 35, −18) and (26, 35, −21)]. The lateral OFC is presumed to provide a value representation, regardless of stimulus modality, and even

Table 3. Metrics characterizing the fMRI activations at the individual level obtained in the two conditions of acquisition, LR and HR.

Brain region	t-test (PSC)	PSC				t-test (baseline)	Baseline				t-test (noise)	Noise			
		HR		LR			HR		LR			HR		LR	
		Mean	SD	Mean	SD		Mean	SD	Mean	SD		Mean	SD	Mean	SD
L Amygdala	p < 0,001	1.57	0.49	1.13	0.60	p < 0,05	1.23	0.08	1.14	0.12	NS	1.10	0.19	1.10	0.16
R Amygdala	p < 0,01	1.34	0.41	1.01	0.45	p < 0,05	1.17	0.12	1.11	0.12	NS	1.18	0.20	1.21	0.26
L Frontal Mid Orb	p < 0,005	2.20	0.90	1.57	0.76	p < 0,0001	1.74	0.41	1.44	0.42	p < 0,001	1.83	0.59	2.29	0.80
R Frontal Mid Orb	NS	2.36	1.09	2.15	1.21	p < 0,0001	1.45	0.35	1.19	0.36	NS	1.72	0.60	1.85	0.66
L Insula	p < 0,0001	1.21	0.20	0.68	0.27	NS	1.60	0.13	1.61	0.13	NS	1.37	0.36	1.33	0.25
R Insula	p < 0,0001	1.27	0.26	0.67	0.30	NS	1.63	0.14	1.62	0.13	NS	1.46	0.31	1.47	0.23

doi:10.1371/journal.pone.0141358.t003

for stimuli that were merely imagined [48–51]. That is why the lateral OFC responds to viewing rewarding food pictures, but the detection of any activity is difficult because of the close air-tissue interfaces. The magnetic susceptibility differences between air and soft tissues create magnetic field gradients around the frontal sinuses, and thus signal dropouts [52, 53]. Other drawbacks come from the poor quality of spatial normalization due to more marked spatial distortions, or the spatial variability of stimulus-specific responses, reflecting inter-subject differences of the affective value when viewing the food images [54]. It is worth noting that the right activation is much weaker than the left one (*i.e.* reduced volume and higher Q_{FDR}). It is therefore likely that the bilateral detection may occur because of the increase in BOLD sensitivity due to the HR condition. A quite similar point is the finding that bilateral activation is restored using HR in the amygdala, while the meta-analyses report only the activation in the left side. The amygdala is known to play a role in reward processing, and its activation by appetizing food images has been observed in subjects with enhanced motivation due to hunger [14, 18]. As for the lateral OFC, it is known that the detection of activation in this region is complicated by the presence of a magnetic field gradient [55]. Our experimental results confirm the earlier suggestion of Merboldt *et al.* [56] that reliable BOLD fMRI of the amygdala requires voxel sizes of 4–8 μl or less. Finally, our study emphasizes that food images in fact elicit bilateral activations in the brain, and that acquiring HR data allows such patterns to be revealed.

It has been shown in [29] that the activations mainly occurred in the left hemisphere. Our results are in line with this observation, and show that the number of significantly activated voxels reaches ~66% in the left hemisphere under both LR and HR conditions. At first sight, this seems to support the valence asymmetry hypothesis of emotion, which posits that the left hemisphere is dominant for positive and the right for negative emotions [57]. Nevertheless, there has not so far been clear-cut evidence for a systematic left-dominance, the region considered [58] and factors such as gender [59] influencing the dominance. Furthermore, the lateralization of activations may also be influenced by methodological artifacts, as previously observed in amygdala [60].

Activations of both the middle and the anterior parts of the insular cortex in response to viewing food pictures were detected under both conditions, but only HR allowed activation of the insular cortex to be observed bilaterally. The first cluster obtained with HR intercepts the part of the anterior insula which overlies the frontal operculum. The second one shows two distinct parts in the middle insula which overlies the Rolandic operculum. Notably, this corresponds with the precise description of gustatory representation within insula obtained by meta-analysis [48]. The activation of the insula found is in line with its responsiveness to most

of the food-related stimuli. In addition to the representation of the gustatory aspects of intra-oral stimuli, the insular taste cortex may have other small functions [61, 62], such as evaluating the biological significance of these stimuli [63]. In sum, finding a bilateral activation in HR of both the posterior and the anterior parts is not surprising, but attributing specific functions to the activated sub-regions remains doubtful.

The activation of the visual system is explained by a stronger elicitation by food than by non-food images, probably because of a greater attentional or motivational salience of food objects (18, 19).

At the individual level, our results (Table 3) emphasize, firstly, that the PSC is significantly higher under HR condition, probably due to the partial volume effect. Indeed, the mixing of active tissues with non-active ones is less likely for a lower voxel volume. In addition, the significant increases of the baseline signal are explained by the reduction of inhomogeneity-induced signal de-phasing due to smaller voxels. This interpretation is corroborated by previous studies which reported the singular amplitude of susceptibility gradients in amygdala [64] and in OFC [65]. We do not highlight important differences of noise levels between the conditions (only a unilateral reduction in the lateral OFC). A 32-channel head coil was used in our study, which is theoretically more sensitive than the 16-channel one used by Bodurka *et al.* [12]. It is thus likely that the voxel volume that splits the thermal noise and physiological noise dominant regimes at 3 T in our experimental conditions may be lower than 5.8 μl for gray matter. Hence the physiological noise may still be dominant using a voxel volume of 3.4 μl, which could explain the slightly different noise levels when comparing LR and HR conditions.

We observe also at the individual level that the across-subject variance on the volume of activation were salient, in agreement with the previous results obtained from a test-retest experiment [66]. This poor reproducibility doubtlessly explains why the mean volume of the activations did not significantly differ between the two conditions LR and HR (data not shown). However, comparing these volumes between individuals, a significant correlation between the two conditions was found, which confirms a reduction in the volume of activations in HR relative to LR, probably because of a lower partial volume effect. Our study indicates that the improvement of sensitivity due to smaller voxel volume has multiple causes and is region-dependent. Indeed, the SNR enhancement due to the mitigation of susceptibility artefact is significant only in regions where the amplitude of magnetic field gradients leads to substantial signal loss (*e.g.* OFC). In regions not prone to such losses, the sensitivity of PSC to the partial volume effect is sufficient justification for acquiring data in HR, especially when the CNR is low. Moreover, the HR condition offers a greater possibility of adapting the width of the smoothing kernel to the true size of activation and to the contrast-to-noise ratio (31), both being unknown. Using HR data and small smoothing kernel width, our results highlight rather small but bilateral and significant clusters in the lateral OFC, the insula and the amygdala (see Table 2 and Fig 3). Most of these activations were observed at HR overlap with already identified taste-responsive regions [48], which supports the involvement of the gustatory cortex when viewing food images, *i.e.* even in the absence of a chemosensory stimulus.

Because many voxels are not prone to vascular effects at 3T and thus have spatial specificity matching the voxel size [2], we can be quite confident about the location of the obtained clusters. Our results suggest that it would be appropriate to reduce further the volume of voxels for obtaining images less prone to physiological noise throughout the brain. However, with single-shot 2D EPI, increasing the spatial resolution lengthens the time necessary to cover a given brain volume. This can be explained (i) by the lengthening of the sampling trajectory, which must traverse an enlarged k-space, and (ii) by the reduction of the slice thickness, which requires a corresponding increase in the number of slices needed. The simplest solution is to increase the acquisition time, which has the drawback of reducing the density of the temporal

sampling. Many other solutions have been developed to improve the spatial resolution without having to degrade the temporal resolution, such as simultaneous multi-slice excitation with multiband radiofrequency pulses [67], parallel imaging [68] or partial-Fourier acquisition [69]. We can expect these developments to continue in this domain owing to constantly improving sensitivity, which allows simultaneous advance in sensitivity and in functional specificity.

Conclusion

Our results demonstrate that acquisition with a voxel volume of 3.4 μl at 3 T leads to a better detection of activations in response to viewing pictures of food compared with the common voxel volume of 27 μl. On the basis of a single group-study using 20 subjects, the regions in which the activations were detected using high spatial resolution gradient-echo EPI were notably consistent with those reported in two activation likelihood estimation meta-analyses. Furthermore, frontal and temporal taste-responsive regions (*i.e.* OFC, amygdala), known to suffer from severe susceptibility artifacts, were found activated bilaterally, that contrasts with previous findings. Such sensitive detection was obtained by optimizing the smoothing size to take more account of partial volume effects, which greatly affect fMRI performance.

Acknowledgments

The study was conducted at IVIA, the *in vivo* multimodal imaging platform of UdA Clermont-Ferrand University (http://www.u-clermont1.fr/).

Author Contributions

Conceived and designed the experiments: JI JMB. Performed the experiments: JI BC BJ. Analyzed the data: JI GM JMB. Contributed reagents/materials/analysis tools: JI GM BC BJ JMB. Wrote the paper: JI GM JMB.

References

1. Newton AT, Rogers BP, Gore JC, Morgan VL. Improving measurement of functional connectivity through decreasing partial volume effects at 7 T. Neuroimage. 2012; 59(3):2511–7. doi: 10.1016/j.neuroimage.2011.08.096 PMID: 21925611; PubMed Central PMCID: PMC3254819.
2. Olman CA, Yacoub E. High-field FMRI for human applications: an overview of spatial resolution and signal specificity. The open neuroimaging journal. 2011; 5:74–89. doi: 10.2174/1874440001105010074 PMID: 22216080; PubMed Central PMCID: PMC3245408.
3. Robinson SD, Pripfl J, Bauer H, Moser E. The impact of EPI voxel size on SNR and BOLD sensitivity in the anterior medio-temporal lobe: a comparative group study of deactivation of the Default Mode. MAGMA. 2008; 21(4):279–90. Epub 2008/07/29. doi: 10.1007/s10334-008-0128-0 PMID: 18661163.
4. Morawetz C, Holz P, Lange C, Baudewig J, Weniger G, Irle E, et al. Improved functional mapping of the human amygdala using a standard functional magnetic resonance imaging sequence with simple modifications. Magn Reson Imaging. 2008; 26(1):45–53. doi: 10.1016/j.mri.2007.04.014 PMID: 17574366.
5. Wildenberg JC, Tyler ME, Danilov YP, Kaczmarek KA, Meyerand ME. High-resolution fMRI detects neuromodulation of individual brainstem nuclei by electrical tongue stimulation in balance-impaired individuals. Neuroimage. 2011; 56(4):2129–37. doi: 10.1016/j.neuroimage.2011.03.074 PMID: 21496490; PubMed Central PMCID: PMC3105209.
6. Frahm J, Merboldt KD, Hanicke W. Functional MRI of human brain activation at high spatial resolution. Magn Reson Med. 1993; 29(1):139–44. PMID: 8419736.
7. Merboldt K-D, Finsterbusch J, Frahm J. Reducing Inhomogeneity Artifacts in Functional MRI of Human Brain Activation—Thin Sections vs Gradient Compensation. Journal of Magnetic Resonance. 2000; 145(2):184–91. doi: 10.1006/jmre.2000.2105 PMID: 10910686
8. Young IR, Cox IJ, Bryant DJ, Bydder GM. The benefits of increasing spatial resolution as a means of reducing artifacts due to field inhomogeneities. Magn Reson Imaging. 1988; 6(5):585–90. PMID: 3226241.

9. Krüger G, Glover GH. Physiological noise in oxygenation-sensitive magnetic resonance imaging. Magnetic resonance in medicine. 2001; 46(4):631–7. PMID: 11590638
10. Triantafyllou C, Hoge RD, Krueger G, Wiggins CJ, Potthast A, Wiggins GC, et al. Comparison of physiological noise at 1.5 T, 3 T and 7 T and optimization of fMRI acquisition parameters. NeuroImage. 2005; 26(1):243–50. doi: 10.1016/j.neuroimage.2005.01.007 PMID: 15862224
11. Triantafyllou C, Hoge RD, Wald LL. Effect of spatial smoothing on physiological noise in high-resolution fMRI. Neuroimage. 2006; 32(2):551–7. doi: 10.1016/j.neuroimage.2006.04.182 PMID: 16815038.
12. Bodurka J, Ye F, Petridou N, Murphy K, Bandettini PA. Mapping the MRI voxel volume in which thermal noise matches physiological noise—implications for fMRI. Neuroimage. 2007; 34(2):542–9. PMID: 17101280
13. Simmons WK, Martin A, Barsalou LW. Pictures of appetizing foods activate gustatory cortices for taste and reward. Cereb Cortex. 2005; 15(10):1602–8. doi: 10.1093/cercor/bhi038 PMID: 15703257.
14. LaBar KS, Gitelman DR, Parrish TB, Kim YH, Nobre AC, Mesulam MM. Hunger selectively modulates corticolimbic activation to food stimuli in humans. Behavioral neuroscience. 2001; 115(2):493–500. PMID: 11345973.
15. Killgore WD, Young AD, Femia LA, Bogorodzki P, Rogowska J, Yurgelun-Todd DA. Cortical and limbic activation during viewing of high- versus low-calorie foods. Neuroimage. 2003; 19(4):1381–94. PMID: 12948696.
16. Killgore WD, Yurgelun-Todd DA. Developmental changes in the functional brain responses of adolescents to images of high and low-calorie foods. Developmental psychobiology. 2005; 47(4):377–97. doi: 10.1002/dev.20099 PMID: 16284969.
17. Rothemund Y, Preuschhof C, Bohner G, Bauknecht HC, Klingebiel R, Flor H, et al. Differential activation of the dorsal striatum by high-calorie visual food stimuli in obese individuals. Neuroimage. 2007; 37 (2):410–21. doi: 10.1016/j.neuroimage.2007.05.008 PMID: 17566768.
18. Beaver JD, Lawrence AD, van Ditzhuijzen J, Davis MH, Woods A, Calder AJ. Individual differences in reward drive predict neural responses to images of food. The Journal of neuroscience: the official journal of the Society for Neuroscience. 2006; 26(19):5160–6. doi: 10.1523/JNEUROSCI.0350-06.2006 PMID: 16687507.
19. Cornier MA, Salzberg AK, Endly DC, Bessesen DH, Rojas DC, Tregellas JR. The effects of overfeeding on the neuronal response to visual food cues in thin and reduced-obese individuals. PLoS One. 2009; 4 (7):e6310. doi: 10.1371/journal.pone.0006310 PMID: 19636426; PubMed Central PMCID: PMC2712682.
20. Cornier MA, Von Kaenel SS, Bessesen DH, Tregellas JR. Effects of overfeeding on the neuronal response to visual food cues. The American journal of clinical nutrition. 2007; 86(4):965–71. PMID: 17921372.
21. Fuhrer D, Zysset S, Stumvoll M. Brain activity in hunger and satiety: an exploratory visually stimulated FMRI study. Obesity (Silver Spring). 2008; 16(5):945–50. doi: 10.1038/oby.2008.33 PMID: 18292747.
22. Schienle A, Schafer A, Hermann A, Vaitl D. Binge-eating disorder: reward sensitivity and brain activation to images of food. Biological psychiatry. 2009; 65(8):654–61. doi: 10.1016/j.biopsych.2008.09.028 PMID: 18996508.
23. Santel S, Baving L, Krauel K, Munte TF, Rotte M. Hunger and satiety in anorexia nervosa: fMRI during cognitive processing of food pictures. Brain Res. 2006; 1114(1):138–48. doi: 10.1016/j.brainres.2006.07.045 PMID: 16919246.
24. Miller JL, James GA, Goldstone AP, Couch JA, He G, Driscoll DJ, et al. Enhanced activation of reward mediating prefrontal regions in response to food stimuli in Prader-Willi syndrome. Journal of neurology, neurosurgery, and psychiatry. 2007; 78(6):615–9. doi: 10.1136/jnnp.2006.099044 PMID: 17158560; PubMed Central PMCID: PMC2077944.
25. Holsen LM, Zarcone JR, Thompson TI, Brooks WM, Anderson MF, Ahluwalia JS, et al. Neural mechanisms underlying food motivation in children and adolescents. Neuroimage. 2005; 27(3):669–76. doi: 10.1016/j.neuroimage.2005.04.043 PMID: 15993629; PubMed Central PMCID: PMC1535274.
26. Davids S, Lauffer H, Thoms K, Jagdhuhn M, Hirschfeld H, Domin M, et al. Increased dorsolateral prefrontal cortex activation in obese children during observation of food stimuli. International journal of obesity. 2010; 34(1):94–104. doi: 10.1038/ijo.2009.193 PMID: 19806158.
27. Malik S, McGlone F, Bedrossian D, Dagher A. Ghrelin modulates brain activity in areas that control appetitive behavior. Cell Metab. 2008; 7(5):400–9. doi: 10.1016/j.cmet.2008.03.007 PMID: 18460331.
28. Tang DW, Fellows LK, Small DM, Dagher A. Food and drug cues activate similar brain regions: A meta-analysis of functional MRI studies. Physiology & Behavior. 2012; 106(3):317–24. doi: 10.1016/j.physbeh.2012.03.009

29. van der Laan LN, de Ridder DT, Viergever MA, Smeets PA. The first taste is always with the eyes: a meta-analysis on the neural correlates of processing visual food cues. Neuroimage. 2011; 55(1):296–303. doi: 10.1016/j.neuroimage.2010.11.055 PMID: 21111829.

30. St-Onge MP, Sy M, Heymsfield SB, Hirsch J. Human cortical specialization for food: a functional magnetic resonance imaging investigation. The Journal of nutrition. 2005; 135(5):1014–8. PMID: 15867274.

31. Davids S, Lauffer H, Thoms K, Jagdhuhn M, Hirschfeld H, Domin M, et al. Increased dorsolateral prefrontal cortex activation in obese children during observation of food stimuli. IntJObes(Lond). 2010; 34 (1):94–104.

32. Uher R, Treasure J, Heining M, Brammer MJ, Campbell IC. Cerebral processing of food-related stimuli: effects of fasting and gender. Behav Brain Res. 2006; 169(1):111–9. doi: 10.1016/j.bbr.2005.12.008 PMID: 16445991.

33. Schur EA, Kleinhans NM, Goldberg J, Buchwald D, Schwartz MW, Maravilla K. Activation in brain energy regulation and reward centers by food cues varies with choice of visual stimulus. International journal of obesity. 2009; 33(6):653–61. doi: 10.1038/ijo.2009.56 PMID: 19365394; PubMed Central PMCID: PMC2697279.

34. Porubska K, Veit R, Preissl H, Fritsche A, Birbaumer N. Subjective feeling of appetite modulates brain activity: an fMRI study. Neuroimage. 2006; 32(3):1273–80. doi: 10.1016/j.neuroimage.2006.04.216 PMID: 16815041.

35. Simmons WK, Martin A, Barsalou LW. Pictures of appetizing foods activate gustatory cortices for taste and reward. CerebCortex. 2005; 15(10):1602–8.

36. Frank S, Laharnar N, Kullmann S, Veit R, Canova C, Hegner YL, et al. Processing of food pictures: influence of hunger, gender and calorie content. Brain Res. 2010; 1350:159–66. doi: 10.1016/j.brainres.2010.04.030 PMID: 20423700.

37. Stoeckel LE, Weller RE, Cook EW 3rd, Twieg DB, Knowlton RC, Cox JE. Widespread reward-system activation in obese women in response to pictures of high-calorie foods. Neuroimage. 2008; 41(2):636–47. doi: 10.1016/j.neuroimage.2008.02.031 PMID: 18413289.

38. Soltysik DA, Hyde JS. High spatial resolution increases the specificity of block-design BOLD fMRI studies of overt vowel production. Neuroimage. 2008; 41(2):389–97. doi: 10.1016/j.neuroimage.2008.01.054 PMID: 18387825; PubMed Central PMCID: PMC2483239.

39. Weibull A, Gustavsson H, Mattsson S, Svensson J. Investigation of spatial resolution, partial volume effects and smoothing in functional MRI using artificial 3D time series. Neuroimage. 2008; 41(2):346–53. doi: 10.1016/j.neuroimage.2008.02.015 PMID: 18400520.

40. Morgan JF, Reid F, Lacey JH. The SCOFF questionnaire: assessment of a new screening tool for eating disorders. Bmj. 1999; 319(7223):1467–8. PMID: 10582927; PubMed Central PMCID: PMC28290.

41. Ashburner J. A fast diffeomorphic image registration algorithm. Neuroimage. 2007; 38(1):95–113. Epub 2007/09/01. doi: 10.1016/j.neuroimage.2007.07.007 PMID: 17761438.

42. Worsley KJ, Friston KJ. Analysis of fMRI time-series revisited—again. Neuroimage. 1995; 2(3):173–81. doi: 10.1006/nimg.1995.1023 PMID: 9343600.

43. Heller R, Stanley D, Yekutieli D, Rubin N, Benjamini Y. Cluster-based analysis of FMRI data. Neuroimage. 2006; 33(2):599–608. doi: 10.1016/j.neuroimage.2006.04.233 PMID: 16952467.

44. Woo CW, Krishnan A, Wager TD. Cluster-extent based thresholding in fMRI analyses: pitfalls and recommendations. Neuroimage. 2014; 91:412–9. doi: 10.1016/j.neuroimage.2013.12.058 PMID: 24412399.

45. Tzourio-Mazoyer N, Landeau B, Papathanassiou D, Crivello F, Etard O, Delcroix N, et al. Automated anatomical labeling of activations in SPM using a macroscopic anatomical parcellation of the MNI MRI single-subject brain. Neuroimage. 2002; 15(1):273–89. doi: 10.1006/nimg.2001.0978 PMID: 11771995.

46. Fransson P, Merboldt KD, Petersson KM, Ingvar M, Frahm J. On the effects of spatial filtering—a comparative fMRI study of episodic memory encoding at high and low resolution. Neuroimage. 2002; 16 (4):977–84. PMID: 12202085.

47. Lieberman MD, Cunningham WA. Type I and Type II error concerns in fMRI research: re-balancing the scale. Soc Cogn Affect Neurosci. 2009; 4(4):423–8. doi: 10.1093/scan/nsp052 PMID: 20035017; PubMed Central PMCID: PMC2799956.

48. Veldhuizen MG, Albrecht J, Zelano C, Boesveldt S, Breslin P, Lundström JN. Identification of human gustatory cortex by activation likelihood estimation. Human Brain Mapping. 2011; 32(12):2256–66. doi: 10.1002/hbm.21188 PMID: 21305668

49. Kühn S, Gallinat J. The neural correlates of subjective pleasantness. NeuroImage. 2012; 61(1):289–94. doi: 10.1016/j.neuroimage.2012.02.065 PMID: 22406357

50. Grabenhorst F, Rolls ET. Value, pleasure and choice in the ventral prefrontal cortex. Trends in cognitive sciences. 2011; 15(2):56–67. doi: 10.1016/j.tics.2010.12.004 PMID: 21216655

51. Cunningham WA, Johnsen IR, Waggoner AS. Orbitofrontal cortex provides cross-modal valuation of self-generated stimuli. Soc Cogn Affect Neurosci. 2011; 6(3):286–93. doi: 10.1093/scan/nsq038 PubMed Central PMCID: PMC3110428. PMID: 20453039

52. Devlin JT, Russell RP, Davis MH, Price CJ, Wilson J, Moss HE, et al. Susceptibility-Induced Loss of Signal: Comparing PET and fMRI on a Semantic Task. NeuroImage. 2000; 11(6):589–600. doi: 10.1006/nimg.2000.0595 PMID: 10860788

53. Ojemann JG, Akbudak E, Snyder AZ, McKinstry RC, Raichle ME, Conturo TE. Anatomic localization and quantitative analysis of gradient refocused echo-planar fMRI susceptibility artifacts. Neuroimage. 1997; 6(3):156–67. PMID: 9344820

54. Rolls ET. Functions of the orbitofrontal and pregenual cingulate cortex in taste, olfaction, appetite and emotion. Acta physiologica Hungarica. 2008; 95(2):131–64. doi: 10.1556/APhysiol.95.2008.2.1 PMID: 18642756.

55. Chen NK, Dickey CC, Yoo SS, Guttmann CR, Panych LP. Selection of voxel size and slice orientation for fMRI in the presence of susceptibility field gradients: application to imaging of the amygdala. Neuroimage. 2003; 19(3):817–25. Epub 2003/07/26. PMID: 12880810.

56. Merboldt KD, Fransson P, Bruhn H, Frahm J. Functional MRI of the human amygdala? Neuroimage. 2001; 14(2):253–7. doi: 10.1006/nimg.2001.0802 PMID: 11467900.

57. Wager TD, Phan KL, Liberzon I, Taylor SF. Valence, gender, and lateralization of functional brain anatomy in emotion: a meta-analysis of findings from neuroimaging. NeuroImage. 2003; 19(3):513–31. doi: 10.1016/S1053-8119(03)00078-8 PMID: 12880784

58. Beraha E, Eggers J, Hindi Attar C, Gutwinski S, Schlagenhauf F, Stoy M, et al. Hemispheric Asymmetry for Affective Stimulus Processing in Healthy Subjects–A fMRI Study. PLoS ONE. 2012; 7(10).

59. Stevens JS, Hamann S. Sex differences in brain activation to emotional stimuli: a meta-analysis of neuroimaging studies. Neuropsychologia. 2012; 50(7):1578–93. doi: 10.1016/j.neuropsychologia.2012.03.011 PMID: 22450197.

60. Mathiak KA, Zvyagintsev M, Ackermann H, Mathiak K. Lateralization of amygdala activation in fMRI may depend on phase-encoding polarity. Magnetic Resonance Materials in Physics, Biology and Medicine. 2011; 25(3):177–82. doi: 10.1007/s10334-011-0285-4

61. {Small S, D. M. Taste representation in the human insula. Brain Struct Funct. 2010; 214(5–6):551–61. doi: 10.1007/s00429-010-0266-9 PMID: 20512366.

62. Rolls ET. Taste, olfactory, and food reward value processing in the brain. Prog Neurobiol. 2015; 127–128:64–90. doi: 10.1016/j.pneurobio.2015.03.002 PMID: 25812933.

63. Araujo I, Geha P, Small D. Orosensory and Homeostatic Functions of the Insular Taste Cortex. Chemosensory Perception. 2012; 5(1):64–79. doi: 10.1007/s12078-012-9117-9 PMID: 25485032

64. Chen N-K, Dickey CC, Yoo S-S, Guttmann CRG, Panych LP. Selection of voxel size and slice orientation for fMRI in the presence of susceptibility field gradients: application to imaging of the amygdala. NeuroImage. 2003; 19(3):817–25. doi: 10.1016/S1053-8119(03)00091-0 PMID: 12880810

65. Tomasi DG, Wang R. Induced magnetic field gradients and forces in the human head in MRI. Journal of Magnetic Resonance Imaging. 2007; 26(5):1340–5. PMID: 17969175

66. Soltysik DA, Thomasson D, Rajan S, Gonzalez-Castillo J, DiCamillo P, Biassou N. Head-repositioning does not reduce the reproducibility of fMRI activation in a block-design motor task. NeuroImage. 2011; 56(3):1329–37. doi: 10.1016/j.neuroimage.2011.03.023 PMID: 21406235

67. Moeller S, Yacoub E, Olman CA, Auerbach E, Strupp J, Harel N, et al. Multiband multislice GE-EPI at 7 tesla, with 16-fold acceleration using partial parallel imaging with application to high spatial and temporal whole-brain fMRI. Magnetic Resonance in Medicine. 2010; 63(5):1144–53. doi: 10.1002/mrm.22361 PMID: 20432285

68. Pruessmann KP, Weiger M, Scheidegger MB, Boesiger P. SENSE: sensitivity encoding for fast MRI. Magnetic resonance in medicine 1999; 42(5):952–62. PMID: 10542355.

69. Hyde JS, Biswal BB, Jesmanowicz A. High-resolution fMRI using multislice partial k-space GR-EPI with cubic voxels. Magn Reson Med. 2001; 46(1):114–25. PMID: 11443717